J Mater Sci: Mater Med (2009) 20:113–122
DOI 10.1007/s10856-008-3547-6

# Use of tissue transglutaminase and fibronectin to influence osteoblast responses to tricalcium phosphate scaffolds

**M. D. Ball · D. O'Connor · A. Pandit**

Received: 18 February 2008 / Accepted: 16 July 2008 / Published online: 14 August 2008


**Abstract** To explore the possibility of controlling cell interaction with biomaterials, tricalcium phosphate scaffolds were modified using the enzyme tissue transglutaminase (tTgase) in conjunction with fibronectin. Previous reports in the literature have highlighted a number of favourable responses that this protein–enzyme complex can stimulate, including enhancing both cell adhesion, and mineralisation. Fibronectin and tTgase alone were used as controls, and a series of different concentrations of tTgase and fibronectin in combination were assessed. Cell metabolic activity, alkaline phosphatase production, and collagen content were all measured in cultures up to 28 days. Using tetracycline labelling, calcium containing multilayered regions were imaged and quantified. Addition of 6 μg fibronectin resulted in increased alkaline phosphatase activity in all combinations, while increased transglutaminase resulted in more collagen in the cell lysates. Samples treated with fibronectin produced many small mineralised areas, those with 6 μg fibronectin and transglutaminase produced numerous large mineralised areas. The mixture of fibronectin and transglutaminase may prove to be a useful treatment for producing increased osteoblast differentiation on scaffolds.

M. D. Ball (✉) · D. O'Connor
National Centre for Biomedical Engineering Science,
National University of Ireland, Galway, Ireland
e-mail: michael.ball@bbsrc.ac.uk

A. Pandit
Department of Mechanical and Biomedical Engineering,
National University of Ireland, Galway, Ireland

*Present Address:*
M. D. Ball
Department of Materials, Imperial College, London, UK

## 1 Introduction

The success and failure of materials implanted into the body are influenced by a number of factors, including how proteins adsorb and change their conformation on encountering the implant surface [1]. Attempts to control the protein reactions at the interface have included coating the surface with adhesion proteins [2–4], or impregnating scaffolds with growth factors [5].

The enzyme tissue transglutaminase (tTgase, type II; EC2.3.2.13) plays a role in a number of cellular processes [6], for example associating with proteins such as collagen [7], fibronectin [8], vitronectin [9] and osteopontin [10–12], all of which are involved in osteoblast adhesion and differentiation. It has the capacity to cross-link extracellular matrix proteins by forming $\varepsilon(\gamma$-glutamyl)lysine isopeptide bonds. Additionally, reports have indicated that tTgase acts as a synergistic binding site with fibronectin (Fn) [8] increasing Fn deposition in the extracellular matrix and controlling storage of latent TGF-$\beta$1 complexes [13]. Transglutaminase has been identified in a number of osteoblast cell lines in vitro [14], found in association with terminally differentiated chondrocytes [15], and implicated in regulating matrix mineralisation [16]. Transglutaminase has also been localised to mineralising osteoblasts, associating with osteopontin and increasing its collagen binding properties [11]. This enzyme can therefore fulfil a number of roles, all of which suggest that it would be an interesting candidate as a protein that could be used to coat biomaterials. Additionally, as a calcium dependent enzyme, there

is the potential for synergistic interaction with a calcium phosphate biomaterial.

Transglutaminases have been used in biomaterial applications to both cross-link gelatin networks [17, 18] and to improve short-term cell adhesion to biodegradable polymers [19, 20]. In this study, the enzyme tissue transglutaminase (tTgase) was immobilized on the surface of commercial tricalcium phosphate (TCP) scaffolds. The protocol used to immobilize proteins to the biomaterial surfaces followed the method used by Heath et al. [19], and as in that study fibronectin was used as a carrier for transglutaminase. This combination of enzymes of the transglutaminase family and fibronectin has been reported as influencing cell adhesion and spreading in the short term [8, 13, 19–24], with no data to date as how this might affect later cell activity. Fibronectin itself is known influence osteoblast activity and differentiation through interactions with cell adhesion proteins, the integrins [25–28]. It has been reported, however, that the pathway by which cells adhere to fibronectin bound tissue tTgase is integrin-independent [23], although integrins are involved in adhesion to complexes formed by plasma transglutaminase (factor XIII) in both cell-ECM [24] and cell–cell adhesion [29]. Additionally, in a co-culture model, chondrocyte-derived tTgase stimulated mineralisation in osteoblastic precursors [30], which appeared to be largely due to secreted tTgase, with a lesser contribution through direct contact with the ECM. In these studies, transglutaminase and fibronectin combinations resulted in increased cell spreading on the biomaterial [19, 20]. There was, however, no indication in these previous studies of whether this would lead to increased extracellular matrix formation or mineralisation. The aim of the present study was to examine longer term reactions. We hypothesise that interactions between transglutaminase and bone proteins such as collagen may influence cell responses later in in vitro culture systems in addition to initial adhesion and cell spreading.

An initial coating of fibronectin was applied, followed 24 h later by transglutaminase, suspended in ethylenediamine tetraacetic acid (EDTA) containing buffer to prevent self-crosslinking. The enzyme was cross-linked onto the material over a subsequent 24 h period. The surfaces were seeded with cells. The cells used were from the SaOs-2 cell line, which have been shown to be a suitable model for mineralising osteoblasts [31]. Metabolic activity, alkaline phosphatase activity, total protein and collagen production were measured over 28 days. In in vitro culture systems, the terminal differentiation of the cells is normally characterized by the generation of mineralized multilayers of cells, termed nodules. Cell coverage and morphology was assessed using scanning electron microscopy.

## 2 Methods

### 2.1 Description of scaffolds

A macroporous $\beta$-tricalcium phosphate scaffold (Vitoss®) was used as the substrate. This biomaterial has been previously been shown to be successful in supporting in vivo bone growth [32, 33]. Macroporous $\beta$-tricalcium phosphate (TCP) samples (Vitoss®, Orthovita, Malvern, PA, USA) were provided as foams consisting of 100% tricalcium phosphate sectioned to create samples roughly circular in cross-section $\sim$2 mm thick and 4.5 mm in diameter. X-ray diffraction was performed to confirm the chemical composition of the ceramics.

### 2.2 Immobilisation of transglutaminase and fibronectin to tricalcium phosphate

Samples were sterilised by autoclaving. Immobilization of protein on samples was performed as described by Heath et al. [19]. Initial coating was performed with a 60 µl aliquot containing 6 or 3 µg bovine plasma fibronectin (Sigma, Tallaght, Dublin) in sterile water. The samples were allowed to air-dry overnight in a laminar flow hood. After drying, 6 and 3 µg of transglutaminase (tTgase) (Sigma, T5398) was added in 60 µl aliquots of 5 mM ethylenediaminetetraacetic acid (EDTA). The tTgase was added and allowed to adsorb for 1 h before being rinsed with sterile Tris–HCl buffer. There were 4.6 enzyme units per mg protein, hence $13.8 \times 10^{-3}$ units in 3 µg tTgase. Three micrograms tTgase equated to 0.65 µM and 6 µg to 1.3 µM. For clarity, the amounts of tTgase are referred to in terms of the mass of protein throughout. The resultant combinations of tTgase and Fn are detailed in (Table 1), and referred to as tTgase-Fn throughout (e.g. 3–6 is 3 µg tTgase, 6 µg Fn).

### 2.3 Measurement of transglutaminase activity after adsorption onto scaffolds

Adsorption of tTgase from solution was assessed by measuring the activity of tTgase in solutions before adsorption and in eluents after rinsing unbound tTgase from scaffolds. Wells from a 96 well plate were coated for 16 h at 4°C

**Table 1** The different treatment regimes used to immobilize transglutaminase and fibronectin to tricalcium phosphate scaffolds

| | Fn µg/ml (µM) | | | |
|---|---|---|---|---|
| tTgase µg/ml (µM) | | 0 | 3 | 6 |
| | 0 | – | Fn 3 (6) | Fn 6 (12) |
| | 3 (0.65) | tTgase 3 | 3–3 | 3–6 |
| | 6 (1.3) | tTgase 6 | 6–3 | 6–6 |

with 250 µl of 100 mM Tris–HCl pH 8.5, 10 mg $ml^{-1}$ *N*,*N*′dimethylcasein (Sigma). Plates were then washed twice with phosphate buffered saline (PBS) containing 0.05% Tween 80 and twice with distilled water. Wells were blocked with 250 µl of 100 mM Tris–HCl pH 8.5, 3% BSA and shaken for 30 min at RT. Plates were washed as previously described with an additional final wash with 100 mM Tris–HCl pH 8.5. To each well was added 150 µl of 100 mM Tris–HCl pH 8.5, 13.3 mM DTT, 6.67 mM $CaCl_2$, 0.1 mg $ml^{-1}$ biotin-cadaverine and 50 µl transglutaminase containing solution. Plates were incubated at 37°C for 2 h and the incorporation reaction was terminated by washing as previously described. To each well was added 200 µl 100 mM Tris–HCl pH 8.5 containing 1% BSA and a 1:5,000 dilution extravidin peroxidase. The plates were incubated at 37°C for 45 min and were washed above but with an extra wash of 100 mM sodium acetate at pH 6. Plates were developed by the addition of 200 µl 100 mM sodium acetate pH 6, 310 µM, 3,3′,5,5′-tetramethylbenzidine, 0.0045% $H_2O_2$. Colour development was terminated by the addition of 50 µl 5 M $H_2SO_4$ and absorbance read at 450 nm. The tTgase activity in the solutions before adsorption and in eluents after rinsing were measured and compared.

### 2.4 Seeding and culture of osteoblast-like cells

SaOs-2 osteoblast-like cells (European Collection of Cell Cultures, Porton Down, Salisbury, UK) were added to each well at a seeding density of $2 \times 10^3$ cells $mm^{-2}$ of sample surface. Cells were seeded in RPMI 1640 media supplemented with 10% serum, 50 IU $ml^{-1}$ penicillin, 0.05 mg $ml^{-1}$ streptomycin, 2 mM glutamine (all Gibco BRL), 50 mg $l^{-1}$ ascorbic acid, 10 mM $\beta$-glycerophosphate and 0.01 mM dexamethasone (all Sigma). The ascorbic acid, $\beta$-glycerophosphate and dexamethasone were added as supplements with the intention of stimulating and supporting osteoblastic differentiation and extracellular matrix formation. The samples were maintained in culture conditions at 37°C in a humidified 5% $CO_2$, atmosphere. All samples were performed in triplicate, experiments repeated three times. Data were analyzed using one-or two-way analysis of variance as appropriate.

### 2.5 Measurement of cell metabolic activity using the alamar blue assay

After 7 days of culture the samples were washed in PBS, placed into fresh, sterile wells and a 1 in 10 dilution of alamar Blue dye (Biosource, UK) in Hank's Balanced Salt Solution (GIBCO BRL) added. Alamar Blue is a chemical which incorporates itself into the electron transporter chain in place of molecular oxygen, and generates a fluorescent product as a consequence. Cells cultured on tissue culture plastic were used as positive controls. The plates were incubated for 1 h before the dye was removed, placed into fresh wells, and measured using a microplate fluorescence reader (Flx800, Bio-Tek Instruments Ltd) at 530 nm excitation wavelength and 590 nm emission wavelength. This was repeated at 14 and 28 days. These data were expressed as a fraction of the cell activity measured on tissue plastic and normalised to total DNA.

### 2.6 Measurement of alkaline phosphatase activity

The samples used above were rinsed again in PBS and 500 µl of double distilled water added to each well. The cells were then subjected to a repeated freeze-thaw cycle, performed three times. A 250 µl aliquot was removed from the suspension to which 250 µl of *p*-nitrophenol phosphate in pH 10.4 buffer was added as an alkaline phosphatase substrate (Sigma). The solution was removed after 3 min and the amount of product formed read on a microplate reader using a 405 nm reference and 620 nm measurement wavelengths. Readings taken at 1, 2 and 3 min were used to calculate the generation of product per minute. The values were normalised against total DNA.

### 2.7 Measurement of total DNA

The DNA content of the cell suspensions was measured by measuring the binding of bis-benzamide 33258 to DNA. [34] This molecule will fluoresce on binding to double stranded DNA. Fifty microliters of cell lysate solution was added to 50 µl of a 20 µg $ml^{-1}$ solution of bis-benzamide 33258 in a 96 well plate. The fluorescence of the dye was measured using a microplate fluorescence reader as before at 360 nm excitation and 460 nm emission wavelengths. Values were determined against a standard curve constructed using calf thymus DNA, and displayed as µg/ml DNA. The data generated from this assay were used to normalise cell activity, alkaline phosphatase production and production of collagen I to cell number.

### 2.8 Measurement of total collagen

Cell lysates, obtained by freeze-thaw of the samples as described above were used for measurement of total collagen, using a Sircol assay kit (Biocolor Ltd, Newtownabbey, Northern Ireland). A 50 µl aliquot of cell lysate was added to a 15 ml polypropylene tube, and the total volume adjusted to 100 µl using distilled water. A set of standards were also created using 5, 10, 25 and 50 µg collagen solution, supplied with the kit. One millilitre of Sircol dye solution was added to each tube, and the contents mixed by shaking for 30 min. The tubes were then

centrifuged at 10,000 rpm for 10 min to generate a pellet, and the supernatant removed. One millilitre of the supplied alkali reagent was added to each tube to solubilise the pellet, and after 10 min the 100 µl of each solution placed into a 96 well plate, and the plate read at 450 nm. The data were normalised to total DNA.

### 2.9 Measurement of transglutaminase activity from cell lysates

Transglutaminase activity was measured in cell lysates as described in method 3.

### 2.10 Labeling of calcium using tetracycline

After 27 days, the culture medium was supplemented with 9 µg/ml tetracycline hydrochloride (Sigma–Aldrich). The following day cells were fixed with 4% paraformaldehyde/2% sucrose in 0.01 M, pH 7.4 phosphate buffered saline (all Sigma–Aldrich) then labelled with propidium iodide (Sigma–Aldrich) at a final concentration of 20 µg/ml. Samples were viewed using a Zeiss LSM 510 confocal laser scanning microscope, equipped with a Spectra Physics Ti Sapphire multi-photon laser used at 710 nm wavelength to excite tetracycline labelled calcium at 355 nm. The use of the multi-photon system means that two photons at the higher 710 nm wavelength can excite the fluorophore at the lower wavelength. A second single photon laser was used to excite propidium iodide at 543 nm wavelength. Twenty millimetre thick sections were collected, and the resulting images were processed using the Imagej software package (NIH, USA). The sizes of areas stained with tetracycline were measured as were the number of stained areas on each sample.

### 2.11 Preparation of samples for scanning electron microscopy

After 7, 14 and 28 days cells were removed from media and processed for scanning electron microscopy. Cells were fixed with 2.5% glutaraldehyde in 0.1 M pH 7.4 cacodylate buffer 2 h at RT. They were then dried using a progressive series of alcohols (50%, 65%, 85%, 80%, 90%, 100%), then covered with hexamethyldisilazane (HMDS) for 30 min at RT. Cells were then sputter coated with gold and viewed using a Hitachi S-4700 SEM at 15kv accelerating voltage.

### 2.12 Statistics

Samples were performed in triplicate. Graphs shown are representative of repeated experiments. Data were considered to be significant at $P < 0.05$. Statistics were performed using the SigmaStat statistical package. Statistics performed were two-way analysis of variance in the case of all tTg-Fn samples, and a one-way analysis of variance in the case of tTgase adsorption from solution. Normality and homogeneity of data were analysed prior to ANOVA. Where significant differences were indicated, a Tukey post-test was used to analyse significant differences between all samples, pairwise.

## 3 Results

### 3.1 X-ray diffraction spectra

The peaks generated by X-ray diffraction were characteristic of $\beta$-tricalcium phosphate ($\beta$-TCP) (Fig. 1).

### 3.2 Cell metabolic activity

Cell metabolic activity peaked at day 28 for all samples except 3–6, which peaked at day 14 ($P < 0.05$, two-way ANOVA) (Fig. 2). Activity of cells cultured on the 3–6 samples were higher at day 14 than the tcp control sample, Fn 3 and 3–3.

### 3.3 Alkaline phosphatase production

Alkaline phosphatase activity per cell clearly peaked at day 14 for cells on all scaffolds, then decreased, with the level at day 28 remaining higher than that at day 7 (Fig. 3). Analysis using a two-way ANOVA indicated that this was linked with fibronectin concentration as all samples with

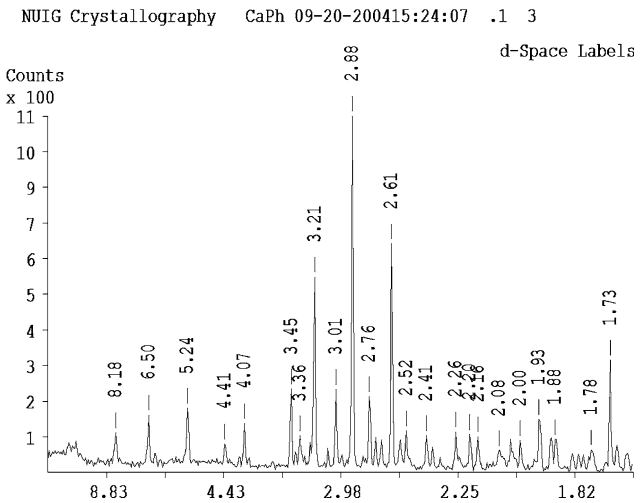


**Fig. 1** X-ray diffraction spectra of calcium phosphate scaffold. The spectra is identified as tricalcium phosphate with no additional phases

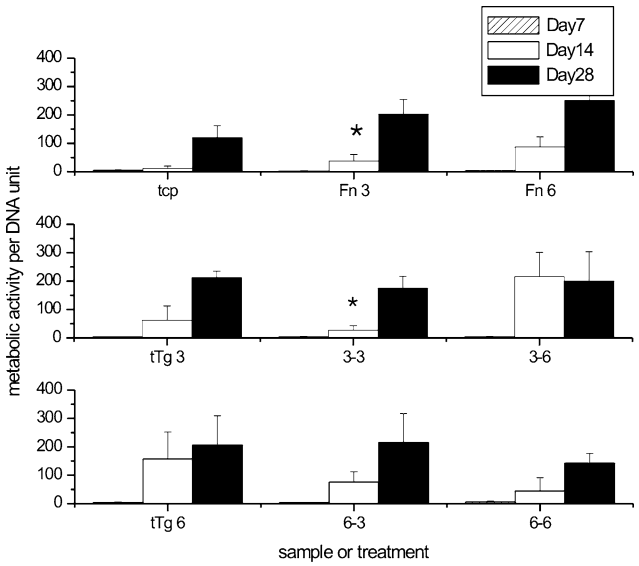


**Fig. 2** Cell metabolic activity per DNA unit as measured by the alamar blue assay. Metabolic activity was divided by total DNA measured from cell lysates. Graph shows activity expressed as a fraction of the control. Activity was measured at 7, 14 and 28 days. Graphs are representative of repeated experiments. Graphs show mean and standard deviation of triplicate samples. Statistics performed were two-way analysis of variance as, $P < 0.05$. Bars marked with * were significantly lower than 3–6 at day 14

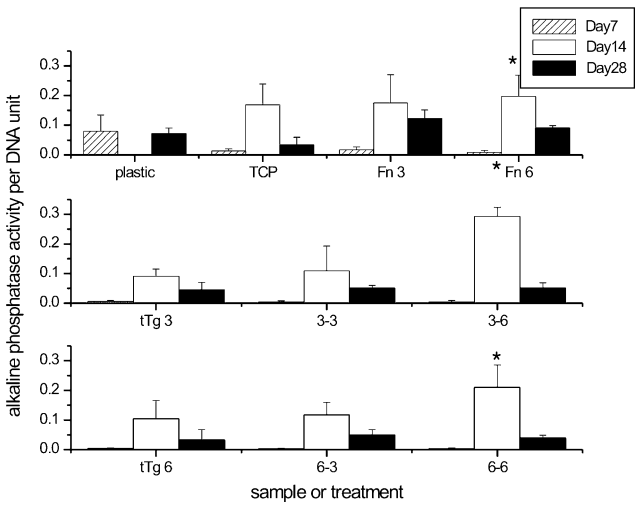


**Fig. 3** Alkaline phosphatase activity per DNA unit as measured using *p*-nitrophenol phosphate. Graph shows enzyme activity expressed as dye conversion per minute (standard international units SIU). Alkaline phosphatase activity was measured in cell lysates at 7, 14 and 28 days. Graphs are representative of repeated experiments. Graphs show mean and standard deviation of triplicate samples. Statistics performed were two-way analysis of variance, $P < 0.05$. *Indicates that samples with 6 μg fibronectin had significantly more alkaline phosphatase activity than those without

6 μg Fn were significantly higher than those with 3 or 0 μg Fn. There were no significant differences between the remaining samples.

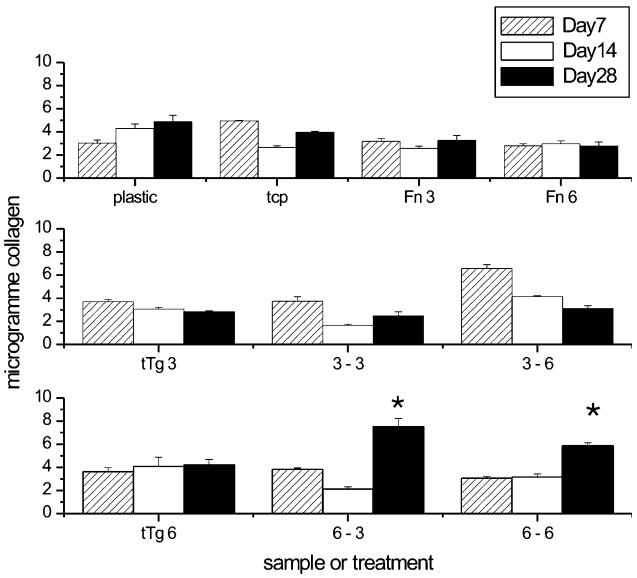


**Fig. 4** Microgrammes collagen in cell lysates, per DNA unit measured using the Sircol assay. Collagen content divided by total DNA measured from cell lysates. Collagen content was measured in cell lysates at 7, 14 and 28 days. Graphs are representative of repeated experiments. Graphs show mean and standard deviation of triplicate samples. Statistics performed were two-way analysis of variance, $P < 0.05$. *Indicate that at 28 days these samples were significantly increased over other samples at the same timepoint

### 3.4 Total DNA

Total DNA measurements were taken for all time points to allow normalisation of samples with respect to cell number. Cell numbers did significantly increase between 7 and 14 days, but showed a significant increase between day 14 and day 28 (data not shown).

### 3.5 Collagen production

Collagen production by cells cultured on all single protein treatments (Fn 3 and 6, tTgase 3 and 6) all showed no significant changes over time. The combinations of tTgase and Fn showed opposite trends depending on the tTgase concentration; 3–3 and 3–6 showed a decrease in collagen, while the 6–3 and 6–6 showed an increase in collagen, with 6–3 and 6–6 both showing increases in collagen from 7 to 28 days, with the collagen at day 28 for both 6–3 and 6–6 being significantly greater than all other combinations (Fig. 4).

### 3.6 Transglutaminase activity in cell lysates

Transglutaminase production was measured in cell lysates as described. Transglutaminase production in cell lysates significantly increased over time, but there was no significant difference between samples (Fig. 5). Transglutaminase

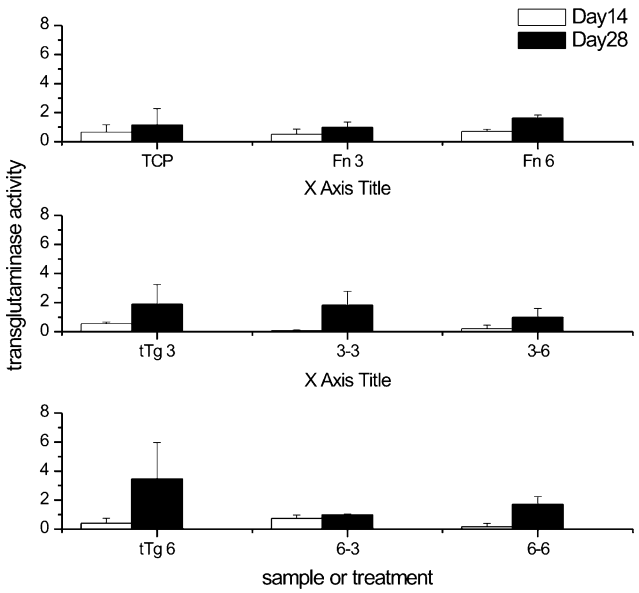


**Fig. 5** Transglutaminase activity in cell lysates, measured using the binding of biotin/cadaverine. Measurements were taken at 7, 14 and 28 days. Graphs are representative of repeated experiments. Graphs show mean and standard deviation of triplicate samples. Statistics performed were two-way analysis of variance, $P < 0.05$

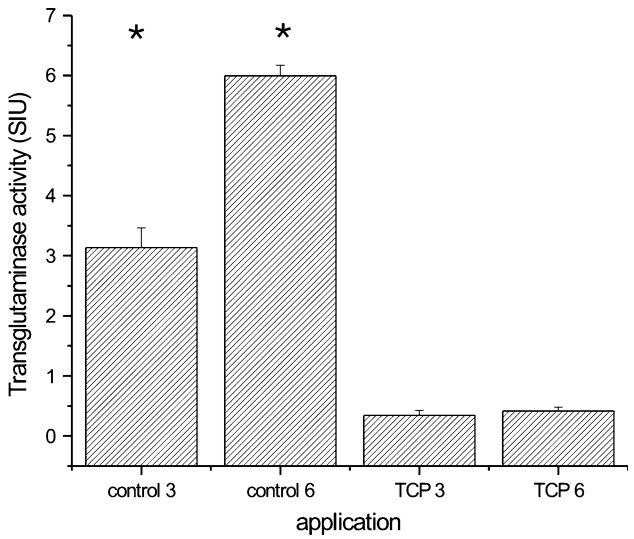


**Fig. 6** Transglutaminase activity in buffer, before and after the application of tTgase to tricalcium phosphate scaffolds, measured using the binding of biotin/cadaverine. Measurements were taken at 7, 14 and 28 days. Graphs are representative of repeated experiments. Graphs show mean and standard deviation of triplicate samples. Statistics performed were a one-way analysis of variance, $P < 0.05$. *Indicate that there was significantly more tTgase activity in solutions prior to addition to the scaffolds

activity in buffer was significantly decreased after addition onto scaffolds, indicating that significant amounts of transglutaminase had bound to the scaffolds (Fig. 6).

### 3.7 Scanning electron micrographs

Cells were visible covering all samples examined. Cells did not cover the entire outer surface of the scaffolds, and the underlying structure was clearly visible on all materials. Large expanses of cells formed sheets of cells that curved across the outside of large pores (<500 μm), and formed multilayered masses in some of the smaller pores (>200 μm). Cells covering the samples treated with Fn alone had large complete expanses of cells, while those on the samples treated with both fibronectin and transglutaminase had sheets of cells, but also smaller conglomerations of rounded cells connected by extracellular matrix proteins (Fig. 7a–i). Numerical calculations of areas covered by cells are given in Table 2.

### 3.8 Tetracycline labelling

Examination of areas of tetracycline labelling revealed variation between samples. The smallest number of stained areas was on the untreated tcp sample, with six stained areas in the field of view analysed. The two tTgase samples, 3 and 6 had 11 and 10 areas respectively, while the two fibronectin coated samples had the largest numbers of stained areas, with Fn 3 having 27 and Fn 6 having 26 areas visible in the fields of view analysed. The size of the stained areas measured on the tcp sample were the smallest of the samples measured with an area of 21.02 ± 6.12 μm, similar in size and number to 3–3 (9 areas, 23.24 ± 3.84 μm). The sample with the largest mean stained areas was the 3–6 combination with a mean area of 47.83 ± 17.42 $\mu m^2$. These figures are summarised in Table 3. Representative images of staining are shown in Fig. 8a and b, with Fig. 8a showing cell nuclei stained using propidium iodide, and 8b showing the equivalent tetracycline staining from these areas.

## 4 Discussion

An essential factor in determining the success or failure of bone-bonding implants is how quickly and effectively bone can form in contact with the material. We used a porous tricalcium phosphate ceramic, confirmed by use of X-ray diffraction, and coated the materials with fibronectin and transglutaminase, confirming transglutaminase adsorption onto the substrates. The pre-adsorption of proteins to the substrate had a significant effect in a number of combinations. Alkaline phosphatase activity per DNA unit peaked at day 14 on all samples, with the highest activity correlating with the highest (6 μg) fibronectin. This peak of alkaline phosphatase activity when normalised to cell

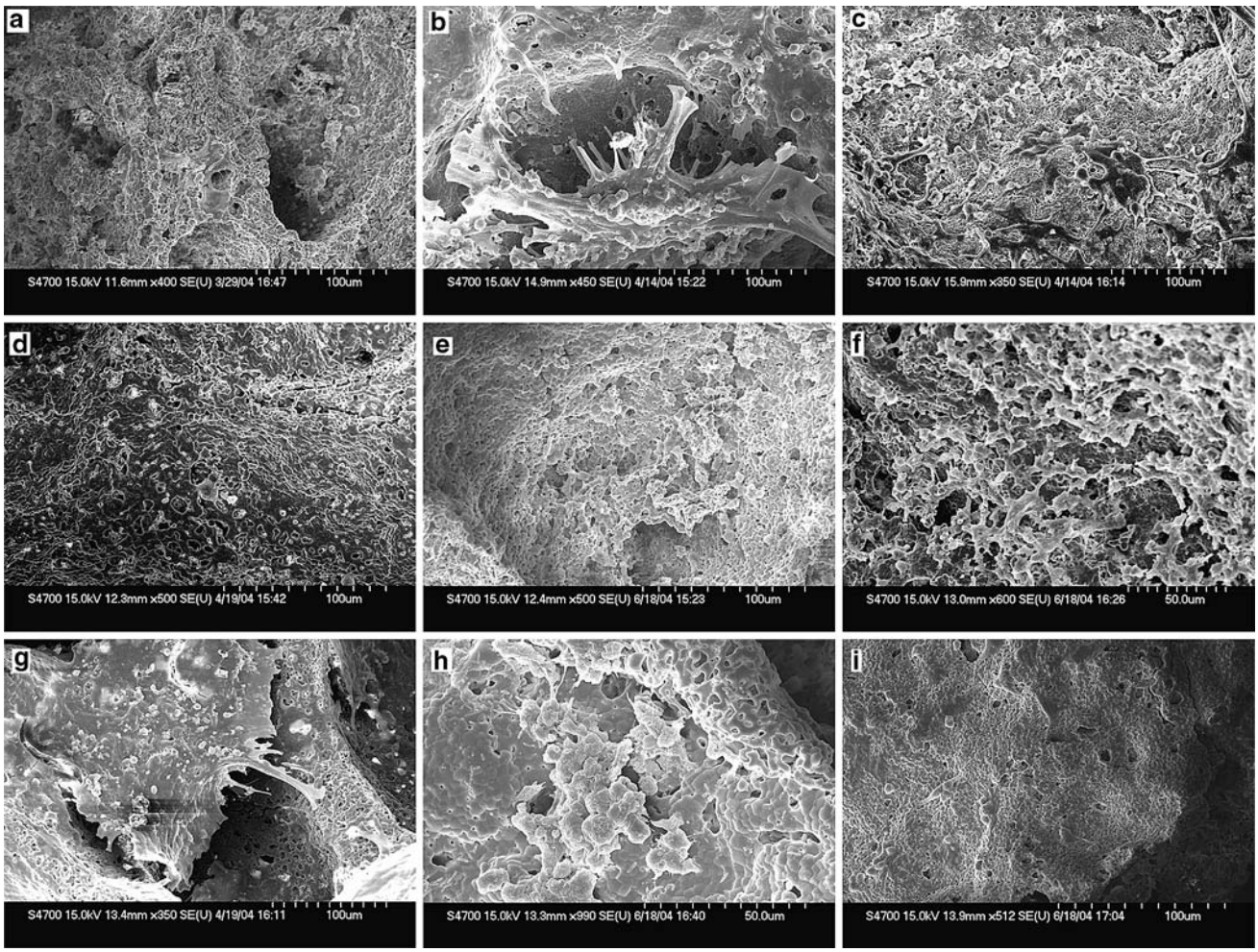


**Fig. 7** Scanning electron micrographs of SaOs-2 osteoblast-like cells after culture on tricalcium phosphate scaffolds. Images were taken at 15 kV accelerating voltage. Images are representative of repeated images. (**a**) Cells cultured on untreated tricalcium phosphate. Cells form patches of monolayers without completely covering the structure. Occasional multilayered regions are visible. (**b**) Cells cultured on tricalcium phosphate with 3 μg immobilized fibronectin. Scaffolds support cells sheets in broken monolayers, with smaller, but more numerous multilayered regions, again occasionally across pores. (**c**) Cells cultured on tricalcium phosphate with 6 μg immobilized fibronectin. Large connecting sheets of cells are visible, again with large numbers of multilayered regions of moderate (30–40 μm) size. (**d**) Cells cultured on tricalcium phosphate with 3 μg immobilized transglutaminase. Cells form discontinuous patches of monolayered cells, which often had multilayered regions associated with them. (**e**) Cells cultured on tricalcium phosphate with 3 μg immobilized transglutaminase and 3 μg immobilized fibronectin. Cells form large patches of monolayered cells, with occasional moderately sized multilayered regions. (**f**) Cells cultured on tricalcium phosphate with 3 μg immobilized transglutaminase and 6 μg immobilized fibronectin. Scaffolds are largely covered by large numbers of cells which form flattened incomplete monolayers with flattened and rounded cells. (**g**) Cells cultured on tricalcium phosphate with 6 μg immobilized transglutaminase. Multilayered regions on these scaffolds were distributed, and associated with shallow pores, but large regions without cells are visible. (**h**) Cells cultured on tricalcium phosphate with 6 μg immobilized transglutaminase and 3 μg immobilized fibronectin. Scaffolds are covered with cell monolayers as well as occasional groups of multilayered rounded cells. (**i**) Cells cultured on tricalcium phosphate with 6 μg immobilized transglutaminase and 6 μg immobilized fibronectin. Cell layers cover large areas of the surface, occasionally covering each other, and forming numerous multilayered 'nodules' but these are relatively small

number is a characteristic indicator of osteoblast differentiation. This is also noted in cell activity, with only the 3–6 combination showing any indicators of an early peak in activity, at 14 days. The strongest link between tTgase and any of the measured factors appeared to be between the two combinations of fibronectin (3 and 6 μg) with 6 μg tTgase, which peaked at day 28, in comparison with all the other combinations of treatments which recorded no change or small decreases. The effect of added fibronectin does not appear to be sustained throughout the culture period. The advantage of pre-coating is maintained up to 14 days, so is not lost due to protein adsorbed from the serum, but might be progressively decreased as the cells secrete fibronectin themselves.

**Table 2** Percentage area of coverage of cells, viewed using the scanning electron microscope

| Sample | Mean %age area of cell coverage (μm) | SD of cell coverage |
|---|---|---|
| TCP only | 262.2 | 6.1 |
| Fn 3 | 34.2 | 15.35 |
| Fn 6 | 58.33 | 13.1 |
| tTgase 3 | 32.1 | 11.47 |
| tTgase 6 | 42.3 | 7.63 |
| 3–3 | 35.61 | 14.66 |
| 3–6 | 34.29 | 9.87 |
| 6–3 | 27.21 | 9.65 |
| 6–6 | 32.88 | 35.76 |

Areas were measured using Imagej image analysis software. Data are mean and standard deviation of areas from three samples

**Table 3** Size and number of tetracycline stained areas per sampled, viewed using the confocal laser scanning microscope

| Sample | Mean area of staining (μm) | SD of staining area | No. of areas |
|---|---|---|---|
| TCP only | 21.02 | 6.12 | 6 |
| Fn 3 | 27.55 | 5.16 | 27 |
| Fn 6 | 36.33 | 11.2 | 26 |
| tTgase 3 | 28.36 | 6.87 | 11 |
| tTgase 6 | 32.3 | 6.64 | 10 |
| 3–3 | 23.24 | 3.84 | 9 |
| 3–6 | 47.83 | 17.42 | 14 |
| 6–3 | 28.66 | 7.07 | 18 |
| 6–6 | 33.02 | 12.02 | 7 |

Areas were measured using Imagej image analysis software. Data are mean and standard deviation of areas from three samples

Hence, we might draw two conclusions; firstly that fibronectin results in differentiation of osteoblasts, and secondly that the activity of transglutaminase either supports increased collagen production, or prevents its breakdown. Transglutaminase has been noted as being involved in extracellular matrix mineralisation, being identified in cartilage matrix in vivo [7, 15] and promotes maturation of osteoblast precursor cells [30]. The extracellular matrix protein measured in this study, collagen, is linked with increasing transglutaminase concentrations at day 28. There is no evidence from this that collagen production itself is increased by transglutaminase, however. Collagen cross-linked by tTgase should be more resistant to degradation and remain after attack by collagenases or matrix metalloproteinases, either produced in culture or released during the freeze-thaw process.

In our culture system, we noted an increase in size and number of mineralized nodules in contact with the samples treated with 3 μg transglutaminase and 6 μg fibronectin (the 3–6 samples). Large numbers of smaller nodules are present on the fibronectin coated samples, while smaller numbers of large nodules are present on the transglutaminase treated sample. This might be a consequence of the enhanced collagen present on the 6–3 and 6–6 samples. The largest nodules are present on the 3–6 sample, which also had a small progressive decrease in collagen. Both

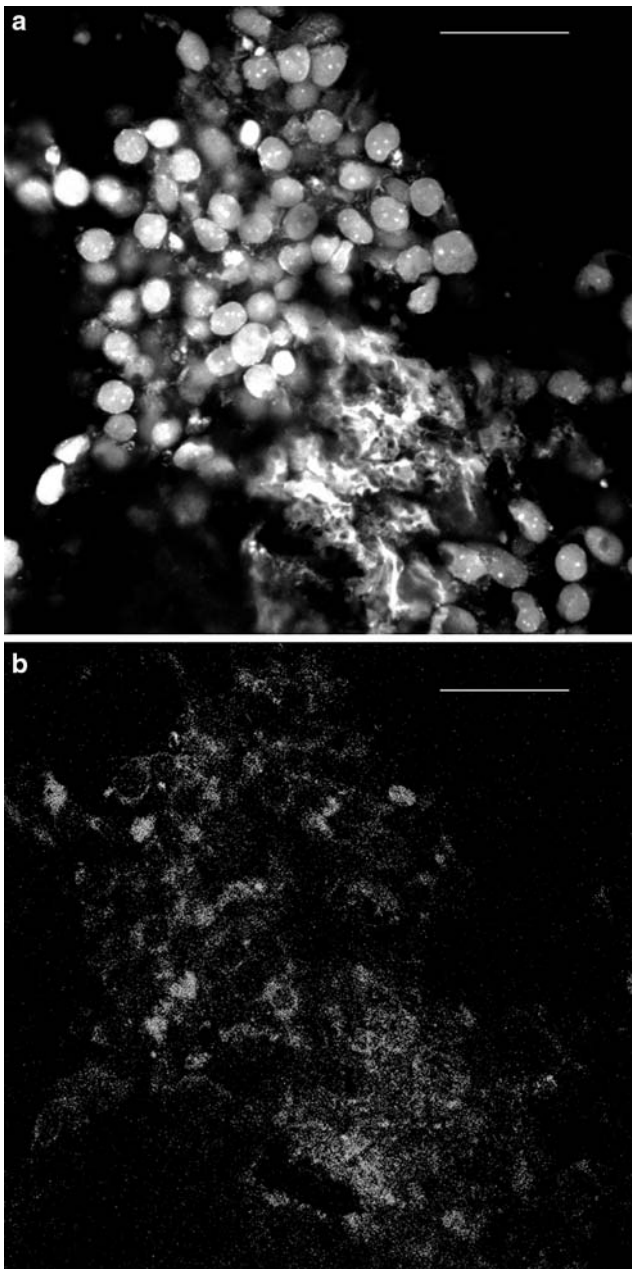


**Fig. 8** Representative confocal laser scanning micrograph of D28 SaOs-2 osteoblasts attached to tricalcium phosphate scaffold. (**a**) Shows cell nuclei stained using propidium iodide and imaged using a 543 nm wavelength laser. (**b**) Shows the same cell mass imaged in (**a**) illuminated using a 710 nm multi-photon laser to excite the tetracycline labelled calcium. The stained areas shown in (**b**) are typical of those measured to generate Table 2

alkaline phosphatase and metabolic data point to the conclusion that the cells on the 3–6 sample had a peak of differentiation around 14 days, hence the change in collagen levels are not likely to be due to loss of phenotype. Instead, we might reasonably conclude that it is instead due to remodelling of the matrix, which could facilitate re-organisation and mineralisation of the matrix. Hence if the matrix is too strongly crosslinked, the remodelling and reorganisation of the matrix might be inhibited, resulting in the small numbers of large nodules we see on the higher concentrations of transglutaminase.

An alternative possibility is that the initially adsorbed transglutaminase stimulated higher production of transglutaminase by the cells themselves, which then acts by crosslinking the extracellular matrix produced by the cells. As there is no significant difference between productions of tTgase on any of the samples, this does not appear to be the case.

In summary, early differentiation is supported by fibronectin, while increased matrix formation or stabilisation is supported by transglutaminase. The largest nodules are found in the combination of 3–6. This is in line with data that suggested a transglutaminase cross-linked extracellular matrix promotes nucleation of mineralisation [16].Samples treated with tTgase and Fn both had numerous, but small nodules, while some low concentrations of tTgase in combination with Fn produced fewer, large nodules.

Applying this type of treatment to a TCP scaffold in a clinical setting might give a different response, as there would be much longer for the adsorbed protein to remain on the substrate before cells colonise the material. However, this would be very useful in a tissue engineered device, producing a stable product with abundant ECM for later cell colonisation.

## 5 Conclusions

1. Transglutaminase is successfully transferred to the tricalcium phosphate scaffold.
2. Fibronectin pre-coated onto the scaffolds increased alkaline phosphatase production at 14 days.
3. 6 μg Transglutaminase in combination with fibronectin resulted in increased collagen after 28 days.
4. The fibronectin coated samples had large numbers of small nodules, the transglutaminase and combination samples had larger nodules. The largest nodules were noted on the 3–6 sample.
5. The combinations of tTgase and Fn are successful in increasing matrix mineralisation by taking advantage of the increased differentiation by Fn and increased matrix stabilization by tTgase.

## References


1. A. El-Ghannam, P. Ducheyne, I.M. Shapiro, J Orthop Res **17**, 340 (1999). doi:10.1002/jor.1100170307
2. U. Geißler, U. Hempel, C. Wolf, D. Scharnweber, H. Worch, K.-W. Wenzel, J Biomed Mater Res **51**, 752 (2000). doi :10.1002/1097-4636(20000915)51:4<752::AID-JBM25>3.0.CO;2-7
3. C. Roehleckea, M. Witta, M. Kaspera, E. Schulzec, C. Wolfb, A. Hofera et al., Cells Tissues Organs **168**, 178 (2001). doi:10.1159/000047833
4. D.M. Ferris, G.D. Moodie, P.M. Dimond, C.W.D. Giorani, M.G. Ehrlich, R.F. Valentini, Biomaterials **20**, 2323 (1999). doi:10.1016/S0142-9612(99)00161-1
5. T.J. Gao, T.S. Lindholm, B. Kommonen, P. Ragni, A. Paronzizni, T.C. Lindholm et al., J Biomed Mater Res **32**, 505 (1996). doi :10.1002/(SICI)1097-4636(199612)32:4<505::AID-JBM2>3.0.CO;2-V
6. L. Fesus, M. Piacentini, Trends Biochem Sci **27**, 534 (2002). doi:10.1016/S0968-0004(02)02182-5
7. D. Aeschlimann, O. Kaupp, M. Paulsson, J Cell Biol **129**, 881 (1995). doi:10.1083/jcb.129.3.881
8. S.S. Akimov, D. Krylov, L.F. Fleischman, A.M. Belkin, J Cell Biol **148**, 825 (2000). doi:10.1083/jcb.148.4.825
9. D.C. Sane, T.L. Moser, A.M. Pippen, C.J. Parker, K.E. Achyuthan, G. CS, Biochem Biophys Res Commun **157**, 115 (1988). doi:10.1016/S0006-291X(88)80020-2
10. M.T. Kaartinen, A. Pirhonen, A. Linnala-Kankkunen, P.H. Maenpaa, J Biol Chem **272**, 22736 (1997). doi:10.1074/jbc.272.36.22736
11. M.T. Kaartinen, A. Pirhonen, A. Linnala-Kankkunen, P.H. Maenpaa, J Biol Chem **274**, 1729 (1999). doi:10.1074/jbc.274.3.1729
12. M.T. Kaartinen, S. El-Maadaway, N.H. Rasanen, M.D. McKee, J Bone Miner Res **17**, 2161 (2002). doi:10.1359/jbmr.2002.17.12.2161
13. S.S. Akimov, A.M. Belkin, J Cell Sci **114**, 2989 (2001)
14. D.J. Heath, S. Downes, E.A.M. Verderio, M. Griffin, J Bone Miner Res **16**, 1477 (2001). doi:10.1359/jbmr.2001.16.8.1477
15. D. Aeschlimann, A. Wetterwald, H. Fleisch, M. Paulsson, J Cell Biol **120**, 1461 (1993). doi:10.1083/jcb.120.6.1461
16. D. Aeschlimann, V. Thomazy, Connect Tissue Res **41**, 1 (2000). doi:10.3109/03008200009005638
17. A. Ito, A. Mase, Y. Takizawa, M. Shinkai, H. Honda, K.-I. Hata et al., J Biosci Bioeng **95**, 196 (2003)
18. E.P. Broderick, D.M. O'Halloran, Y.A. Rochev, M. Griffin, R.J. Collighan, A.S. Pandit, J Biomed Mater Res B Appl Biomater **72**, 37 (2005). doi:10.1002/jbm.b.30119
19. D.J. Heath, P. Christian, M. Griffin, Biomaterials **23**, 1519 (2002). doi:10.1016/S0142-9612(01)00282-4
20. E.A.M. Verderio, A. Coombes, R.A. Jones, L. Xiaoling, D.J. Heath, S. Downes et al., J Biomed Mater Res **54**, 294 (2001). doi :10.1002/1097-4636(200102)54:2<294::AID-JBM17>3.0.CO;2-Q
21. C.A. Gaudry, E. Verderio, R.A. Jones, C. Smith, M. Griffin, Exp Cell Res **252**, 104 (1999). doi:10.1006/excr.1999.4633
22. R. Jones, B. Nicholas, S. Mian, P. Davies, M. Griffin, J Cell Sci **110**, 2461 (1997)
23. E.A.M. Verderio, D. Telci, A. Okoye, G. Melino, M. Griffin, J Biol Chem **278**, 42604 (2003). doi:10.1074/jbc.M303303200
24. S. Ueki, J. Takagi, Y. Saito, J Cell Sci **109**, 2727 (1996)
25. A.J. Garcia, D. Boettiger, Biomaterials **20**, 2427 (1999). doi:10.1016/S0142-9612(99)00170-2
26. A.J. Garcia, J. Takagi, D. Boettiger, J Biol Chem **273**, 34710 (1998). doi:10.1074/jbc.273.52.34710
27. A. Moursi, R. Globus, C. Damsky, J Cell Sci **110**, 2187 (1997)

28. S.N. Stephansson, B.A. Byers, A.J. Garcia, Biomaterials **23**, 2527 (2002). doi:10.1016/S0142-9612(01)00387-8
29. R. Dardik, B. Shenkman, I. Tamarin, R. Eskaraev, J. Harsfalvi, D. Varon et al., Thromb Res **105**, 317 (2002). doi:10.1016/S0049-3848(02)00014-2
30. M. Nurminskaya, C. Magee, L. Faverman, T.F. Linsenmayer, Dev Biol **263**, 139 (2003). doi:10.1016/S0012-1606(03)00445-7
31. D.J. McQuillan, M.D. Richardson, J.F. Bateman, Bone **16**, 415 (1995)
32. G. Meadows, Orthopaedics **25**, s579 (2002)
33. R. Linovitz, T. Peppers, Orthopaedics **25**, 585 (2002)
34. R. Rago, J. Mitchen, G. Wilding, Anal Biochem **191**, 31 (1990). doi:10.1016/0003-2697(90)90382-J